5th International Conference on Water Resources and Arid Environments (ICWRAE 5): 264-275
7-9 January 2013, Riyadh, Saudi Arabia

Delineating Groundwater Aquifer and Subsurface Structures Using Integrated Geophysical Interpretation at the Western Part of Gulf of Aqaba, Sinai, Egypt

[1]Sultan Awad Sultan Araffa and [2]Josef Pek

[1]National Research Institute of Astronomy and Geophysics (NRIAG), Helwan, Cairo, Egypt
[2]Institute of Geophysics, Academy of Sciences of Czech Republic

Abstract: Different geophysical tools such as geoelectrical, gravity and magnetic are perfect for delineating the geometry of groundwater aquifer, subsurface structural elements which control the extension and thickness of the aquifer. Also, the seismological data records were used for differentiating the active fault elements in study area. In the present study, 7 deep vertical electrical soundings have been measured by using AB/2 ranging from 5 m to 3000 m to reach the depth of upper and lower surface of the Nubian sandstone aquifer. The results of quantitative interpretation of resistivity data indicated that the depth of the upper surface of Nubian sandstone aquifer was ranging from 366 m to 845 m. Three hundred-thirty gravity stations have been measured to cover the study area. Results of quantitative interpretation indicated that the area was dissected by different fault trends such as NE-SW, NW-SE, N-S and E-W trends. Three hundred-thirty land magnetic stations have been executed and interpreted to detect the basement depth and then the thickness of sedimentary deposits. The results of magnetic interpretation revealed that the depth of basement was ranging from 1243m to 1718 m. Also, One thousand-seventy three earthquake events have been recorded to represent the seismic activity in the study area.

Key words: Groundwater · Gravity · Magnetic and seismicity

INTRODUCTION

The present study is focused on the eastern part of Sinai. Sinai, particularly the Gulf of Aqaba region, is promising for Egypt's economic growth. The only disadvantage for the development of this area is water. The present work aims to estimate the parameters of the deep aquifer (Nubian sandstone aquifer) through the geophysical investigation for the study area and delineating the subsurface structures and their effect on the configuration of the aquifer. Resistivity techniques are well-established and widely used to solve a variety of geotechnical, geological and environmental subsurface detection problems [1, 2, 3]. The surface geophysical methods have been used for aquifer zone delineation and evaluation of the geophysical character of the aquifer zone in several locations [4-16]. The gravity method involves measuring the earth's gravitational field at specific locations on the earth's surface to determine the location of subsurface density variations. The gravity method works when buried objects have different masses, which are caused by the object having a greater or lesser density than the surrounding material. However, the earth's gravitational field measured at the earth's surface is affected also by topographic changes, the earth's shape and rotation and earth tides. These factors must be removed before interpreting gravity data for subsurface features. The final form of the processed gravity data can be used in many types of engineering and environmental problems, including determining the thickness of the surface or near-surface soil layer, changes in water table levels and the detection of buried tunnels, caves, sinkholes and near-surface faults. Also, temporal variations of the gravitational field can be used to determine variations in the water table [17, 18] and changing of subsidence levels in sinkholes. The gravity method can be a relatively easy geophysical technique to perform and interpret. It requires only simple but precise

Corresponding Author: Sultan Awad Sultan Araffa, National Research Institute of Astronomy and Geophysics (NRIAG), Helwan, Cairo, Egypt. E-mail: sultan_awad@yahoo.com.

data processing and for detailed studies the determination of a station's elevation is the most difficult and time-consuming aspect. The technique has good depth penetration when compared to ground penetrating radar, high frequency electromagnetics and DC-resistivity techniques and is not affected by the high conductivity values of near-surface clay rich soils. Additionally, lateral boundaries of subsurface features can be easily obtained especially through the measurement of the derivatives of the gravitational field.

The magnetic method is one of the best geophysical techniques to delineate subsurface structures. Aeromagnetic maps reflect spatial variations in the magnetic field of the earth. These variations are related to distribution of structures, magnetic susceptibilities and/or remnant magnetization. Sedimentary rocks, in general, have low magnetic properties compared with igneous and metamorphic rocks that tend to have a much greater magnetic content [19]. Magnetic method is an important tool to detect the upper surface of the basement and, indirectly, the thickness of the sedimentary cover. Many geophysical investigations have been carried out around the study area. [20, 21] were studied groundwater potentiality at the northern and eastern parts of the study area. The distribution of earthquakes, the understanding of the structure of the mantle of the earth and the availability of kinematic data for the oceanic ridges simplified the construction of global plate tectonic models [22, 23, 24, 25, 26].

Geology of the Area: The study area lies at the east central part of Sinai, located between latitudes 28° 50` and 29° 50` N and longitudes 33° 50` E and 34° 50`, the study area occupies an area of 115x92= 10580 km^2 (Fig. 1). Most of the study area is occupied by high mountains at the eastern and southern part, Egma plateau occupying the western part of the area. The area is dissected by different wadis which people of Bedouins live around them. The topography of the study area is usually high specially at the southwestern part where the elevation is up to 1600 m but the northern and eastern parts reveal moderately elevations around 600m, the west central part and coast area of Aqaba Gulf show low elevation of about 20-140 m (Fig. 2). The surface geology of the study area is described from the geological map of Sinai at a scale of 1:500,000, performed by [27] and is shown in Figure 3. The area is covered by different geologic formations for different geologic ages, where Quaternary deposits represented in the study area by coastal facies at Aqaba Gulf Coast. Pleistocene deposits are represented by

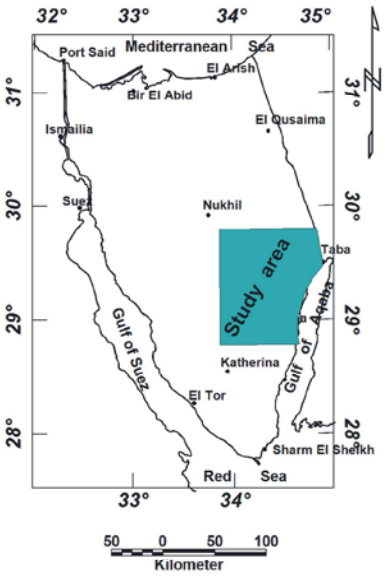

Fig. 1: Location map of the study area

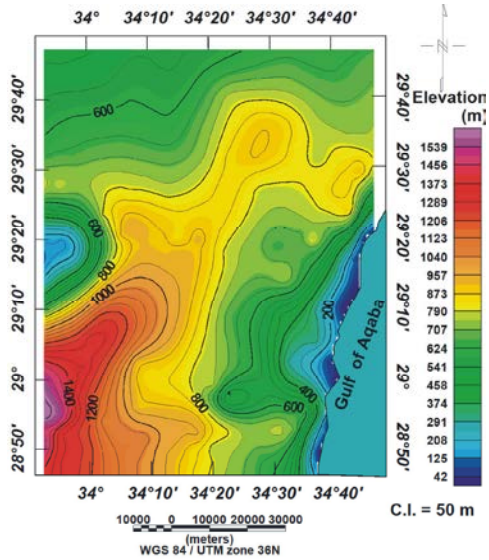

Fig. 2: Topographic map of the study area

alluvial deposits and franglomrates which covered most wadis and distribute through the most area. Paleocene deposits including Esena shale Formation, which is composed of marly shale and located at the northern part of the area. Lower Eocene is represented by two formations the first is the Thebets Formation which is composed of limestone and distributed as patches throughout the area. The second Formation is Egma Formation which consists of chalky limestone and covers most of the study area at the western part. The Upper Cretaceous is represented by Sudr Formation, which is composed of chalk of Maastrichtian age, Duwai Formation

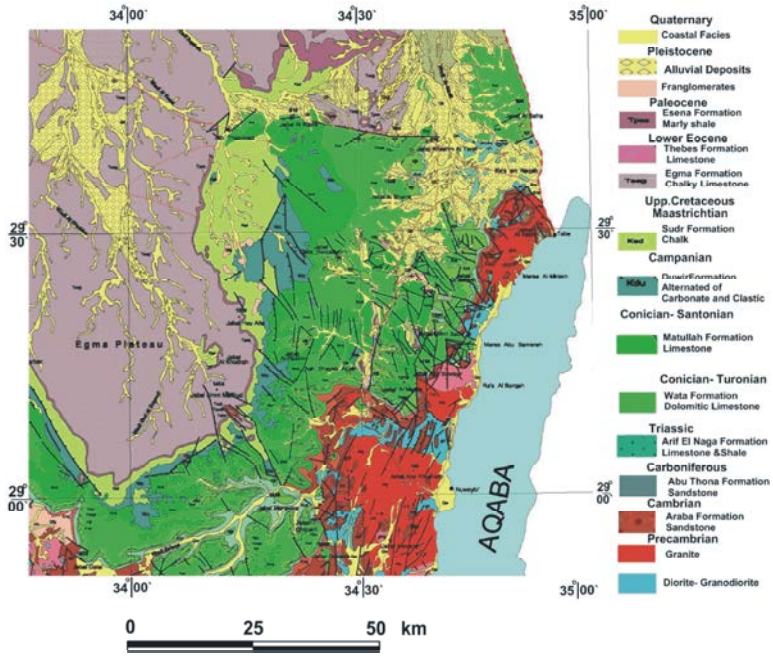

Fig. 3: Geologic map (modified after UNSECO Cairo Office, 2004)

composed of alternated carbonate and clastic of Campanian age, Matullah Formation, which composed of limestone of Conician-Santonian age and Wata Formation composed of dolomitic limestone of Conician-Turonian deposits. The eastern part of the study area is covered by basement rocks of Precambrian age which is composed mainly of granite, diorite and granodiorite.

MATERIALS AND METHODS

Vertical Electrical Sounding (VES): The electrical resistivity of any material depends largely on its porosity and the salinity of the water in the pore spaces. Although the electrical resistivity of a material may not be diagnostic, certain materials have specific ranges of electrical resistivity. In all electrical resistivity surveying techniques, a known electrical current is passed through the ground between two (or more) electrodes. The potential (voltage) of the electrical field resulting from the application of the current is measured between two (or more) additional electrodes at various locations. Since the current is known and the potential can be measured, an apparent resistivity can be calculated. The separation between the current electrodes depends on the type of surveying being performed and the required investigation depth. Electrical resistivity, also referred to as galvanic electrical methods, is occasionally useful for determining shallow and deep geologic and hydrogeologic conditions. The most common array for electrical resistivity surveying in the sounding mode is the Schlumberger array. By increasing the separation of the outer current electrodes, thereby driving the currents deeper into the subsurface increases the depth of exploration. Electrical resistivity sounding surveys measure vertical changes in the electrical properties of subsurface materials. The electrode spacing used for resistivity sounding is variable, with the center point of the electrode array remaining constant. Electrical resistivity data acquired in the sounding mode, using the Schlumberger array, can be modeled using master curves or computer modeling algorithms. When using master curves, the interpreter attempts to match overlapping segments of the apparent electrical resistivity versus electrode separation plots with a succession of two-layer master curves. This modeling method provides coarse estimates of the model parameters, is time consuming and requires skill on the part of the interpreter. There are a variety of different types of algorithms; some assume discrete electrical resistivity layers while others assume that electrical resistivity is a smooth function of depth.

Resistivity Data Acquisition: Seven deep vertical electrical soundings have been measured by [28], Egypt. One of them was carried out beside borehole Jica4 to calibrate the model of resistivity data with results of borehole (Fig. 4). The resistivity data were measured

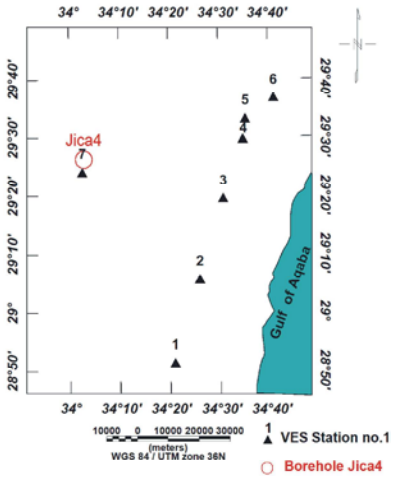

Fig. 4: Location map of VES stations and bore

using the Schlumberger configuration with AB/2 spacing ranging from 5m to 3000 m. The main objective was to detect the Nubian sandstone aquifer in the study area. The data were acquired using the CH-8708A transmitter and the EPR0121A recorder along with the inverted non-linear approach.

Resistivity Data Interpretation: The authors used a manual (graphical) interpretation, which depends upon matching the plotted field curves with the standard curves and the generalized Cagniard graphs [29]. The obtained results of the manual interpretation were used as initial models for the analytical methods. The quantitative interpretation was made using the IPI2WIN program. It has been designed by a scientific group in Moscow State University, Russia in 2010, This program uses a linear filtering approach for the forward calculation of a wide class of geological models depend upon regularized fitting minimizing algorithm using Tikhonov's approach [30, 31, 32]. This program deals with VES curves in man-computer interactive regime and draws theoretical and field curves on a display screen together with Rho (z) model curve. The quantitative interpretation has been applied to determine the thicknesses and true resistivities of the stratigraphic units below each VES stations, as well as, the groundwater content and water quality in the study area. The interpretation is starting with the VES no.7 where the data of borehole Jica4 was calibrated (Fig. 5). The interpretation of the VES no.7 revealed eight geoelectrical units the upper most three units were grouped in one layer called wadi deposits until depth of 30 m according to data of borehole. The second layer which represented the fourth geoelectrical unit was represented by cherty limestone up to depth of 80 m. The third layer was represented by shale layer of low resistivity value. The fourth layer was chalky limestone and shale which has depth ranging from 80 to 110 m. The fifth layer was dolomitic limestone up to depth of 380 m. The sixth layer was the Nubian sandstone aquifer which had depth ranging from 380 to 845 m. These results of resistivity data revealed coincidence with data of borehole. The other six VESes were represented by geoelectrical cross section which included the VESes no.1, 2, 3, 4, 5 and 6. The results of interpretation indicated that the depth reached the upper surface of basement complex at the VESes no.3, 4, 5 and 6. The depth of basement rocks was compare with depth of basement which calculated by gravity interpretation through 3D magnetic modeling. The thickness of the Nubian sandstone aquifer can be executed through subtracting depth of upper surface of Nubian sandstone aquifer from the depth basement rocks. By this way the thickness of the Nubian aquifer was ranging from 900-1000 m (Fig. 6). The values of true resistivity for the Nubian sandstone were relatively moderate indicating the quality of water was good due to salinity was low. The total dissolved salts was 1047 ppm from the chemical analysis of the borehole Jica4.

Gravity Method: Gravity anomalies are the result of contrasts in densities of materials in the Earth. If all the materials within the Earth were layered horizontally and were of uniform density, there would be no density contrasts. Density contrasts of different materials are controlled by a number of different factors; the most important are the grain density of the particles forming the material, the porosity of the material and the interstitial fluids within the material. Generally, soil and shale specific gravities range from 1.7 to 2.2. Massive limestone specific gravities average 2.7. While this range of values may appear to be fairly large, local contrasts will be only a fraction of this range. A common order of magnitude for local density contrasts is 0.25. Density contrasts can be determined by calculating the gravity effect of a known model and comparing that effect with the observed gravity determined from a gravity survey. Gravity surveys provide an inexpensive determination of regional structures that may be associated with groundwater aquifers or petroleum traps. Gravity surveys have been one of the principal exploration tools in regional petroleum exploration surveys. Gravity surveys have somewhat limited applications in geotechnical investigations. Gravity surveys have been used to obtain information on bedrock depths and the top of rock.

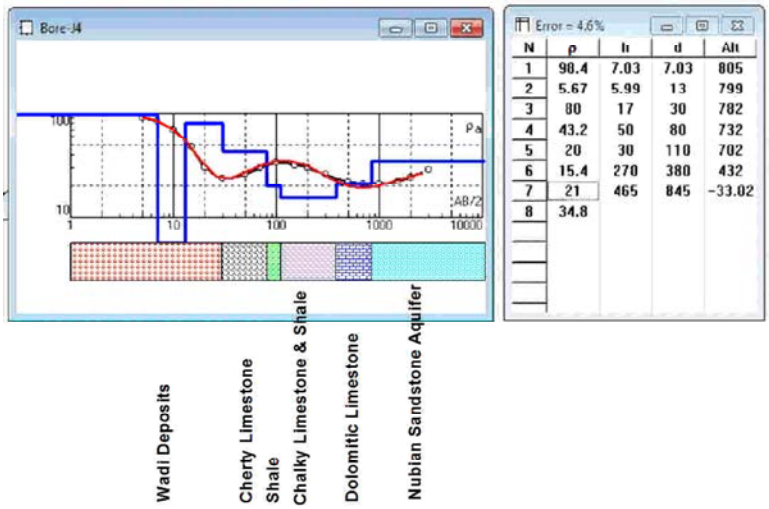

Fig. 5: Interpretation of VES station 7 complied by bore

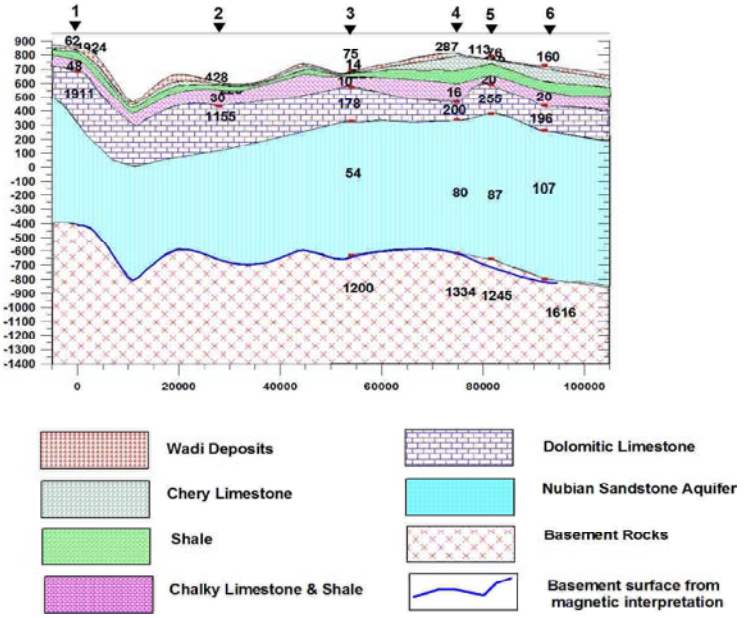

Fig. 6: Geolectrical cross-section along profile A-A

Data Gravity Acquisition: Three hundred-thirty gravity stations had been measured by using Auto-Grav (CG3) gravity meter of sensitivity of 0.01 mGal (Fig. 7). The measured gravity values corrected to different gravity corrections such as, drift, tide, free-air, Bouguer, latitude and topographic corrections. Using specialized Geosoft software [32]. The corrected gravity values were used to plot Bouguer anomaly map using Oasis Montaj, 2007. Bouguer anomaly map (Fig. 8a) exhibited high gravity anomalies at the n orthern and northwestern parts (-17 mGal), but the central, southwestern and costal plain of Gulf of Aqaba parts reveal low gravity anomalies (-62 mGal).

Gravity Separation: The regional- residual separation technique with a cut wave number of 0.02486 km^{-1} are carried out to filter the regional component, which related to deep-seated sources and residual component, which related to local sources. In the present study, authors used low pass and high pass techniques to apply the gravity separation. A high-pass filter sharpens the input data by the application of a convolution filter. The filter is called 'high-pass' because it allows high wave numbers (high frequencies) to pass to the output channel. Features in the data that were longer than the long wavelength cutoff were removed. The convolution filter was designed using the method of Fraser, 1966. The default length will

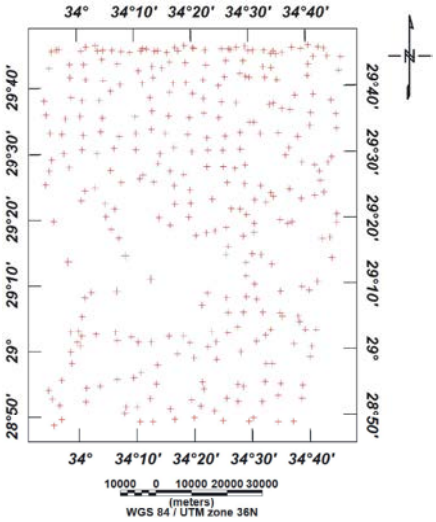

Fig. 7: Location map for gravity and magnetic stations

be as long as the cutoff wavelength, which produces a filter that exhibits a minimum of side effects, such as Gibb's phenomena. The high pass filter (residual) map (Fig. 8b) exhibited different anomalies of low and high amplitudes which were used to define trends. A low-pass filter smoothed the input data by the application of a convolution filter to the data. The filter was called 'low-pass' because it allowed slow wave numbers (low frequencies) to pass to the output channel. Features in the data that were shorter than the short wavelength cutoff were removed. The low pass filter (regional) map (Fig. 8c) revealed high gravity anomaly at the western, northern and eastern parts but the central and costal area along Gulf of Aqaba exhibited low gravity anomaly.

Gravity Interpretation: The interpretation of gravity data had been used to define trends and depths of structural elements which dissect the study area. Euler deconvolution technique was used to apply for the high pass (residual) gravity anomalies. The standard Euler deconvolution, moves a window of a fixed size (10x10) over a grid of data and calculates Euler Deconvolution solutions for each window. There are typically many solutions, virtually one for every window location, which approaches the number of cells in the grid. The apparent depth to the gravity and magnetic sources is derived from Euler's homogeneity equation (Euler deconvolution). This process relates the gravity or magnetic field and its gradient components to the location of the source of an anomaly, with the degree of homogeneity expressed as a "structural index". The structural index (SI) is a measure

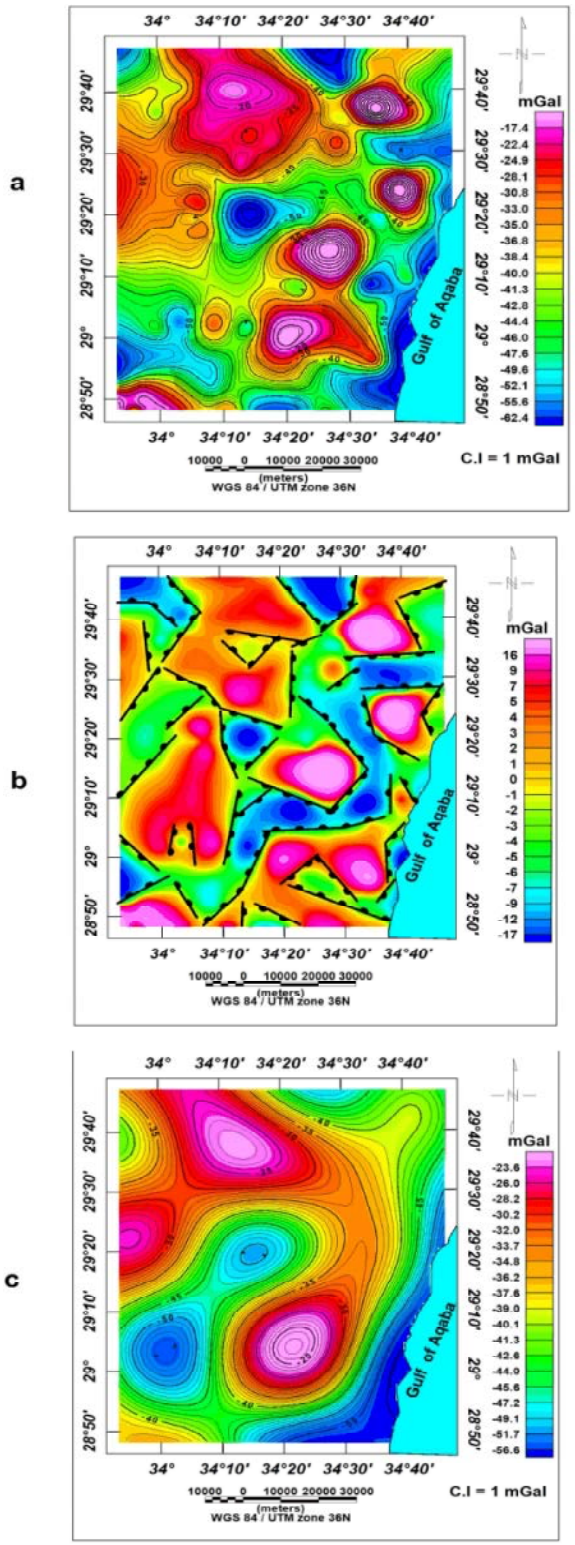

Fig. 8: a: Gravity anomaly map, b: high pass filter (residual) map complied with the fault element traces, c: low pass filter (regional) map

of the fall-off rate of the field with distance from the source. The Euler deconvolution process is applied at each solution. The method involves setting an appropriate SI value and using least-squares inversion to solve the equation for an optimum xo, yo, zo and B. As well, a square window size must be specified which consists of the number of cells in the gridded dataset to use in the inversion at each selected solution location. The window is centred on each of the solution locations. All points in the window are used to solve Euler's equation for solution depth, inversely weighted by distance from the centre of the window. The window should be large enough to include each solution anomaly of interest in the total field gravity or magnetic grid, but ideally not large enough to include any adjacent anomalies. A structural index is an exponential factor corresponding to the rate at which the field falls off with distance, for a source of a given geometry.

From the following table choose an appropriate model for your structural index value.

Gravity Field	Magnetic Field	SI
Sill/Dyke/Ribbon/Step	Contact/Step	0
Cylinder/Pipe	Sill/Dyke	1
Sphere	Cylinder/Pipe	2
N/A	Sphere/Barrel/Ordnance	3

In the present study authors used structural index 0, 0.5 and 1 to select the best solution, (Fig. 9), The Figure 9a of structural index 0 gives better solution than structural index 0.5 and 1, also the figure 9a is similar o fault element which detect from high pass (residual) map.

Magnetic Method: The magnetic method exploits small variations in magnetic mineralogy (magnetic iron and iron-titanium oxide minerals, including magnetite, titanomagnetite, titanomaghemite and titanohematite and some iron sulfide minerals, including pyrrhotite and greigite) among rocks. Magnetic rocks contain various combinations of induced and remnant magnetization that perturb the Earth's primary field [34]. The magnitudes of both induced and remnant magnetization depend on the quantity, composition and size of magnetic-mineral grains. Magnetic anomalies may be related to primary igneous or sedimentary processes that establish the magnetic mineralogy, or they may be related to secondary alteration that either introduces or removes magnetic minerals. Induced magnetic anomalies are the result of secondary magnetization induced in a ferrous body by the earth's magnetic field. The magnetic method is an effective way

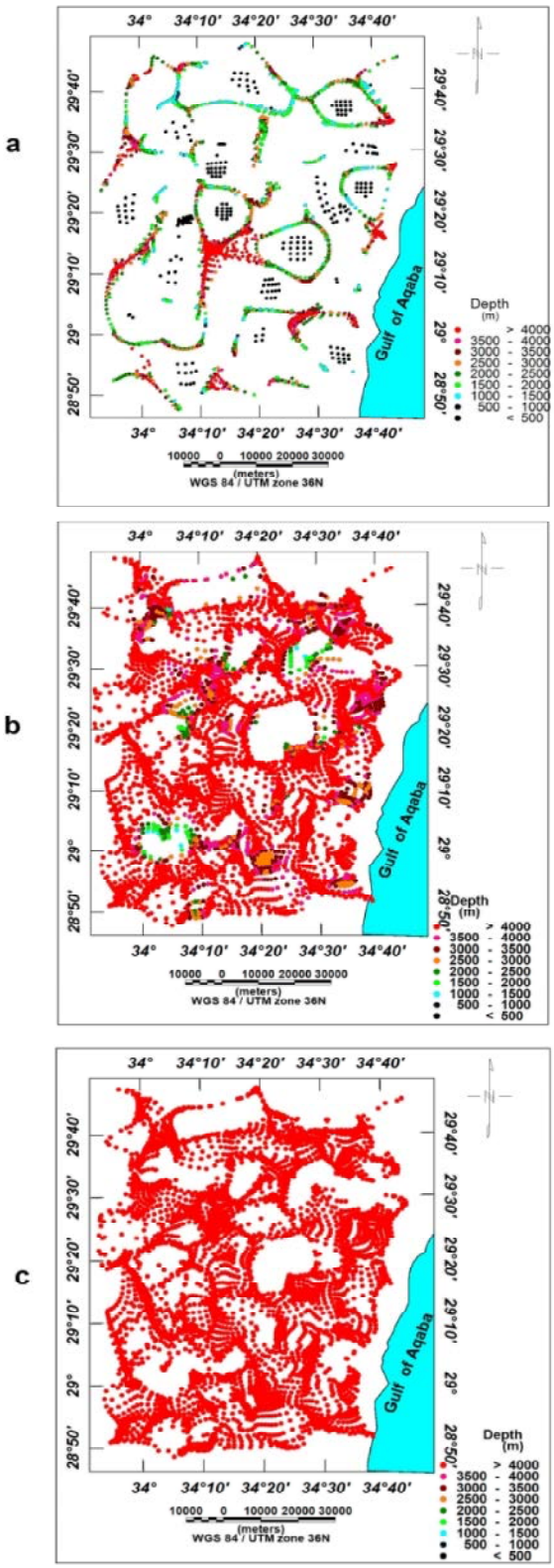

Fig. 9: Euler solutions structural index a: 0 (zero), B: 0.5, c: 1

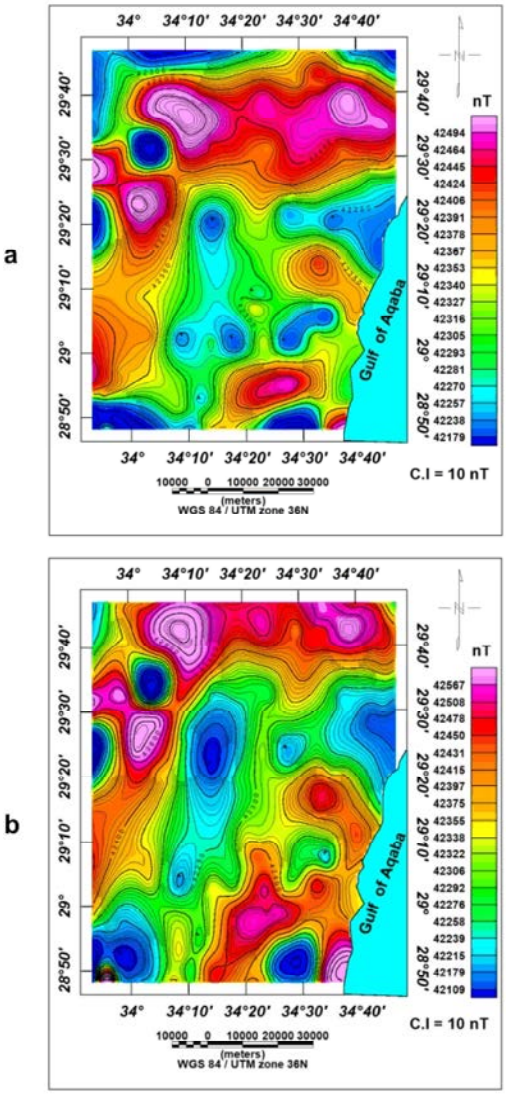

Fig. 10: a:Total intensity magnetic map, b: Total intensity magnetic map reduced to the pole

to search for small metallic objects because magnetic anomalies have spatial dimensions much larger than those of the objects.

Magnetic Data Acquisition: Three hundred-thirty stations of magnetic data had been measured by using two Envimag Proton magnetometers made by Scintrex Company of Canada with one 1 nT sensitivity. The first one was used for the base station recordings to apply the diurnal variation correction and the other one was used for field measurements. The obtained values were corrected for normal gradient of earth magnetic field (IGRF) and diurnal variation corrections, the corrected magnetic values were contoured using Geosoft [33] to be represented by a total intensity magnetic map (Fig. 10a). The total intensity magnetic data were reduced to the magnetic pole to overcome the distortion in the appearance of an anomaly. This appearance depends on the magnetic latitude of the survey area and on the dip angle of the magnetization vector in the body; a mathematical procedure is adopted on a grid of values of the contour map of the total magnetic intensity. This mathematical procedure was first described by Baranov [35, 36, 37, 38]. The total intensity magnetic map after been reduced to the pole (Fig. 10b) indicated that the northern, western and eastern parts of the study area were occupied by high magnetic structures while the central was represented by low magnetic structures.

3-D Magnetic Modeling Interpretation: The aims of magnetic interpretation are determining depth of basement surface and the thickness of the sedimentary rocks. The author used GMSYS-3D software for Oasis Montaj [33] package. GMSYS-3D is a 3D gravity and magnetic modeling package for surface-oriented models. A model is defined by a number of stacked surface grids with density-, susceptibility- and remanent magnetization-distributions specified for the layer below each surface. Calculations were performed in the wave number domain and were based on Dr. Bill Pearson's implementation of R.L. Parker's algorithm [39]. The program was designed to run within Oasis montaj, 2007 making available all of the familiar grid manipulation and display routines in addition to application-specific routines. The results of GMSYS-3D indicated that the calculated magnetic data (RTP) were very similar to the observed magnetic data where the misfit err was ranging between 4 and -7 nT (Fig. 11). The results of 3-D magnetic modeling are presented in Figure 12. The depth of basement surface from the interpretation of magnetic data through 3-D modeling indicated that the depth of basement was ranging from 1243 m at the southern part to 1718 m at the southwestern part of the study area.

Seismology Method: The tectonics of the Sinai Peninsula and the Gulf of Aqaba are strongly dominated by the active boundaries between the African and the Arabian plates which are separating one from the other. The Sinai Peninsula has been recognized as subplate of the African plate located at the triple junction among the Gulf of Suez rift, the Aqaba- Levant transform fault (the southernmost part of the Dead Sea-Jordan transform) and the Red Sea rift [40]. One thousand -eighty earthquakes events had been recorded in the study area, some of these events

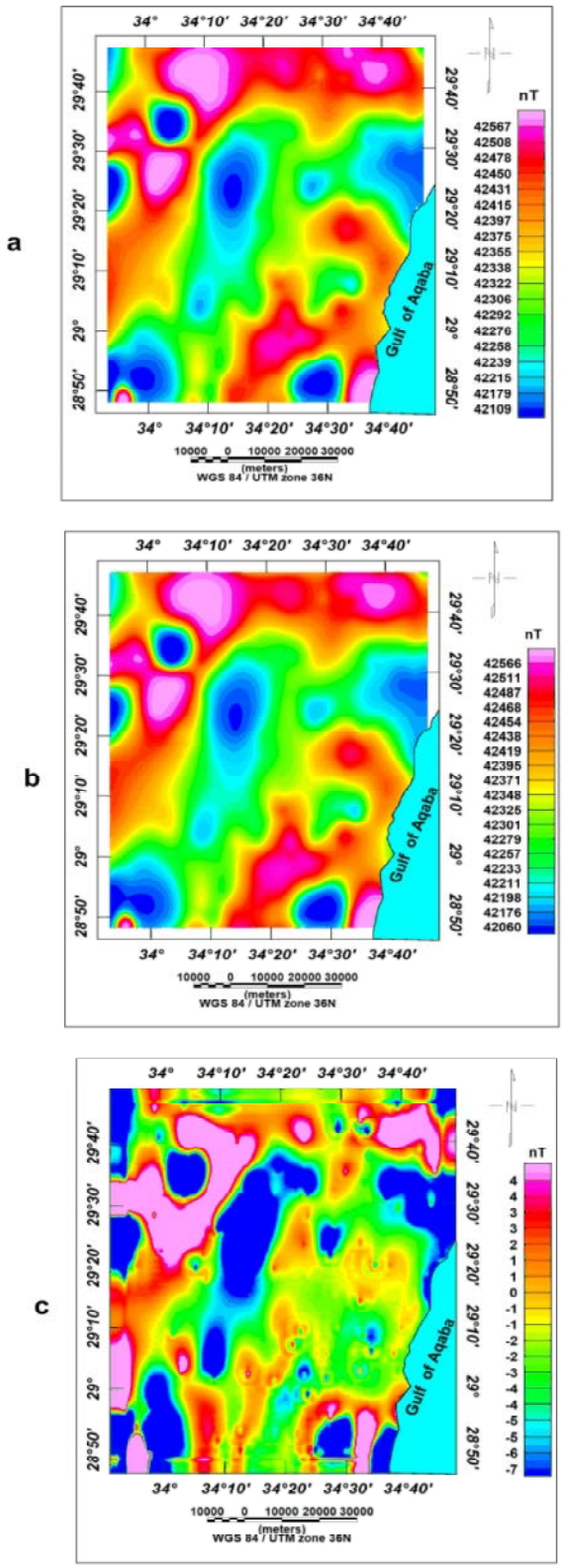

Fig. 11: a: observed magnetic map (RTP), b: Calculated magnetic map, c: misfit error

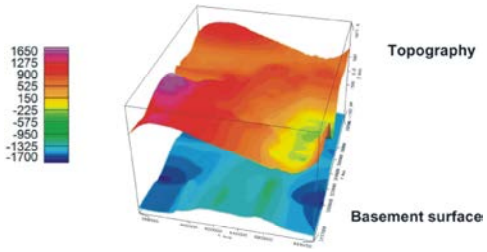

Fig. 12: 3-D magnetic modeling representation

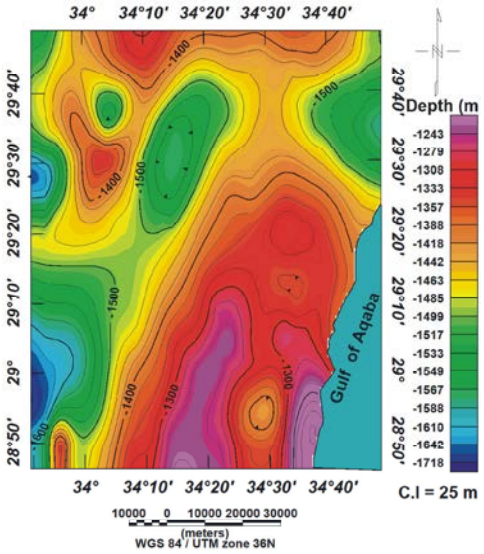

Fig. 13: Depth to the basement surface from 3-D magnetic modeling

were located at the fault elements which indicated that they were active faults. The minimum magnitudes of the earthquake events are about 1 Richter and the maximum magnitude was ranging from 5-6 Richter (Fig. 14a). The depth of the earthquake events was ranging from 1 to more than 20 km and most events laid at depth of 5-10 km (Fig. 14b). Most the earthquake events took place at date of 1990-2000 (Fig. 14c) and indicated that the fault elements which dissected the study area were active faults, also these great number of the events indicated that Sinai is a subplate due to the movement between Arabian plate and Sinai subplate.

DISCUSSION

The study area lies at the east central Sinai,and suffers from scarcity of water resources as it is far from the Nile Valley. This study amis to investigate the deep groundwater aquifer which called Nubian sandstone aquifer. This aquifer is characterized by good quality of water which used for drinking, domestic

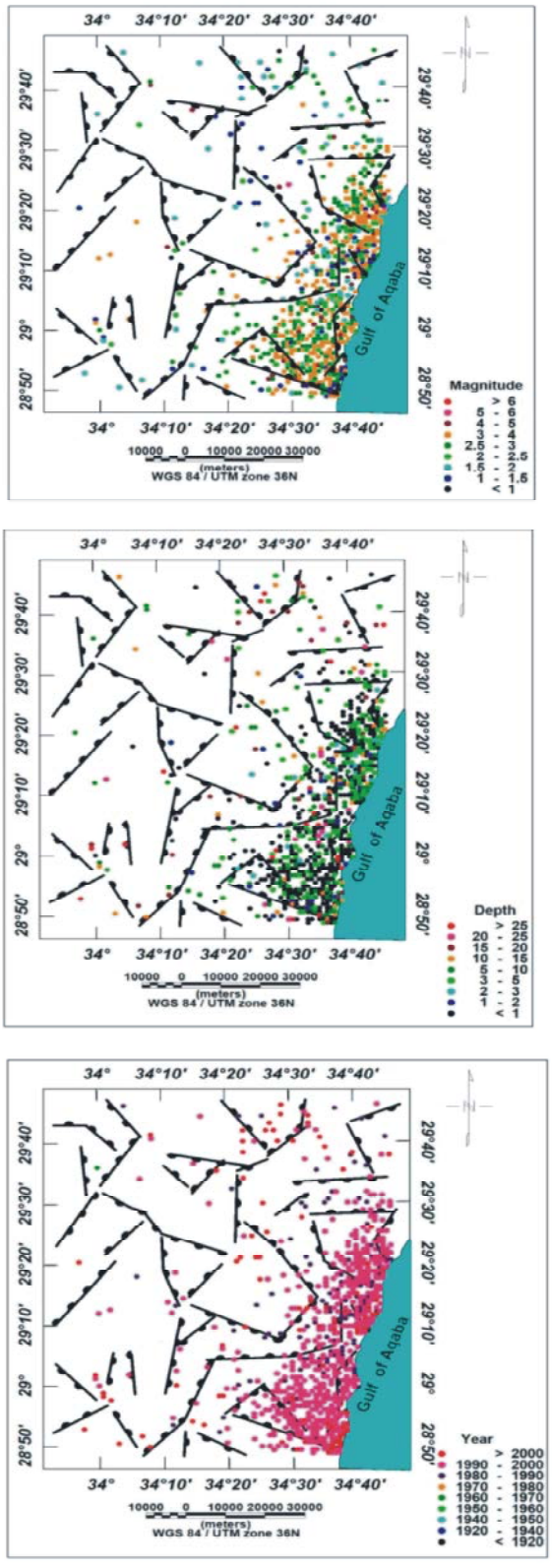

Fig. 14: Earthquake events complied with fault elements location according to gravity interpretation

and agricultural purpose. Integrated geophysical interpretation had been done to evaluate the geometry of this aquifer such as the depth and thickness as well as the water quality. Also, the study aims to delineate the structural element which dissect the study area and detect the active fault element through estimating the seismological history and their effect on the distribution of the population. The interpretation geoelectrical resistivity tool (vertical electrical sounding) showed good correlation between the results of resistivity data and those of borehole Jica4, where the depths of interface between different geological units were coincident, as for example the depth of the upper surface for Nubian sandstone aquifer in borehole Jica4 was 840 m and from resistivity interpretation is 845 m (good agreement). The depth of the lower surface of the Nubian sandstone aquifer from resistivity interpretation was 1323, 1420, 1540 and 1521 m for VESes no.3, 4, 5 and 6 respectively while from magnetion interpretation (3-D magnetic modeling) was 1320, 1422, 1470 and 1540m for VESes no.3, 4, 5 and 6 respectively. The interpretation of gravity data indicated that the area dissected by different fault elements of NW-SE, NE-SW, N-S and E-W trends. These trends coincided with the trends of Gulf of Suez, Gulf of Aqaba, Nile Valley and Mediterranean Sea. Finally the seismological activity in the area indicated the theory of opining the Gulf of Aqaba due the movement between Arabian plate and Sinai subplate.

CONCLUION

From the results of integrated geophysical interpretation on the study area we can concluded that:

- The study area contain deep groundwater aquifer (Nubian sandstone aquifer) at depth ranging from 1323 m to 1540 m and thickness of about 950m.
- The quality of the groundwater is good quality of TDS about 1047 ppm.
- The area dissects by fault elements of trends NW-SE, NE-SW, N-S and E-W, some of them are active faults.
- The area is characterized by high seismic activity due the movement between Arabian plate and Sinai subplate.

REFERENCES

1. Ward, S.H., 1990. Geotechnical and Environmental GeophysicsSeries Investigations in Geophysics, vol. 5. Society of Exploration Geophysics, Tulsa, USA.

2. Sultan, S.A. F.A. Santos and A. Helal, 2006. A study of the Grounwater Seepage on Hibis Temple Using Geoelectrical Data, Kharaga, Egypt, Egypt, near surface geophysics Journal, pp: 347-354.
3. Sultan, S.A., 2010. Geophysical investigation for shallow subsurface geotechnical problems of Mokattam area, Cairo, Egypt, Environmental Earth Sciences Journal, 59: 1195-2207.
4. Ungemach, P., F. Moslaghini and A. Duprat, 1969. Emphasis in determination of transmissivity coefficient and application in nappe alluvial aquifer Rhine. Bult. Instt. Assoc. Sci. Hydrol. XIV(3): 169-190.
5. Kelly, W., 1977. Geoelectric sounding for estimating aquifer hydraulic conductivity. Groundwater, 15(6): 420-425.
6. Heigold, P.C., R.H. Gilkson, K. Cartwright and P.C. Reed, 1979. Aquifer transmissivity from surficial electrical methods. Groundwater, 17: 338-345.
7. Kosinki, W.K. and W.E. Kelly, 1981. Geoelectric soundings for predicting aquifer properties. Groundwater, 19: 163-171.
8. Niwas, S. and O.A.L. De Lima, 2003. Aquifer parameter estimation from surface resistivity data. Groundwater, 41(1): 94-99.
9. Frohlich, R. and W.E. Kelly, 1985. The relation between transmissivity and transverse resistance in a complicated aquifer of glacial outwash deposits. Journal of Hydrology, 79: 215-219.
10. Huntley, D., 1986. Relations between permeability and electrical resistivity in granular aquifers. Groundwater, 24(4): 466-474.
11. Worthington, P.F., 1993. The uses and abuses of the Archie equations: 1. The formation factor-porosity relationship. Journal of Applied Geophysics, 30: 215-228.
12. Frohlich, R.K., J.J. Fisher and E. Summerly, 1996. Electric-hydraulic conductivity correlation in fractured crystalline bedrock: Central landfill, Rhode Island, USA. Journal of Applied Geophysics, 35: 249-259.
13. Yadav, G.S. and H. Abolfazli, 1998. Geoelectrical soundings and their relationship to hydraulic parameters in semiarid regions of Jalore, Northwestern India. Journal of Applied Geophysics, 39: 35-51.
14. Dhakate, R. and V.S. Singh, 2005. Estimation of hydraulic parameters from surface geophysical methods, Kaliapani Ultramafic Complex, Orissa, India. Journal of Environmental Hydrology 13(paper 12).
15. Khalil, M.H., 2006. Geoelectric resistivity sounding for delineating salt water intrusion in the Abu Zanima area, west Sinai, Egypt. Journal of Geophysics and Engineering, 3: 243-251.
16. Pantelis, M., P.M. Soupios, M. Kouli, F. Vallianatos, A. Vafidis and G. Stavroulakis, 2007. Estimation of aquifer hydraulic parameters from surficial geophysical methods: A case study of Keritis Basin in Chania (Crete - Greece), J. Hydrol., 338: 122-131.
17. Mokkapati, S., 1995. Mapping porosity variations using microgravity monitoring in the Blaine aquifer, southwestern Oklahoma: M.S. Thesis, University of Oklahoma, Norman, OK.
18. Hare, J., J. Ferguson, C. Aiken and J. Brady, 1999. The 4-D microgravity method for waterflood surveillance: A model study for the Prudhoe Bay reservoir, Alaska: Geophysics, 64: 78-87.
19. Aboud E., Ahmed, A. Salem and K. Ushijima, 2005. Subsurface structural mapping of Gebel El-Zeit area, Gulf of Suez, Egypt using aeromagnetic data, Earth Planets Space, 57: 755-760.
20. Sultan, S.A. and El A.L. Sorady, 2001. Geoelectric and gravity measurements for groundwater exploration and detection of structural elements at Romana area, Northwest of Sinai, Egypt., in Proceedings of the 6th Conf. Geology of Sinai for Development, Ismailia, pp: 109-120.
21. Monteiro Santos, F.A.M., S.A. Sultan, R. Patrýcia and A.L. El Sorady, 2006. Joint inversion of gravity and geoelectrical data for groundwater and structural investigation: application to the northwestern part of Sinai, Egypt. Geophys. J. Int., 165: 705-718.
22. Wilson J.T., 1965. A new class of faults and their bearing on continental drift Nature, 207: 343-34.
23. Le Pichon X., 1968. Sea-floor spreading and continental drift, J. Geophy. Res., 73: 3661-3677.
24. Chase, C.G., 1978. Plate kinematics: the Americas, East Africa and the rest of the World, Earth and Plan, Sci. Lett., 37: 355-368.
25. Minster, J.B. and H.T. Jordan, 1978. Present-day plate motion. J. Geophy. Res., 83: 5331-5354.
26. Badawy, A. and F. Ferenc Horva'th, 2001. The Sinai subplate and tectonic evolution of the northern Red Sea region, Journal of Geodynamic, 27: 433-450.
27. UNSECO Cairo Office, 2004. Geologic Map of Sinai, Egypt, Scale 1:500,000, Project for the Capacity Building of the Egyptian Geological survey and Mining Authority and the National Authority for Remote Sensing and Space Science in Cooperation with UNDP and UNSECO., Geological Survey of Egypt.

28. Water Resources Research Institute and Japan International Cooperation Agency,1999. South Sinai groundwater resources study in the Arab Republic of Egypt. Main Rep, WRRI, El-Kanater El Khayria.
29. Koefoed, O., 1960. A generalized Cagniard graph for interpretation of geoelectric soundingdata. Geophysical Prospecting, 8(3): 459-469.
30. Bobachev, A., I. Modin and V. Shevnin, 2001. IPI2WIN v.2.0, User's Manual.
31. Gian, P.D., B. Ernesto and M. Cristina, 2003. Inversion of electrical conductivity data with Tikhonov regularization approach: some considerations, Annals of Geophysics, 46(3).
32. Chuansheng, W., H. Jinrong and Z. Xiufen, 2008. AGenetic AlgorithmApproach for Selecting Tikhonov Regularization Parameter, IEEE Congress on Evolutionary Computation (CEC 2008).
33. Geosoftw Program (Oasis Montaj), 2007. Geosoft mapping and application system, Inc, Suit 500, Richmond St. West Toronto, ON Canada N5SIV6.
34. Reynolds, R.L., J.G. Rosenbaum, M.R. Hudson and N.S. Fishman, 1990, Rock magnetism, the distribution of magnetic minerals in the Earth's crust and aeromagnetic anomalies, in Hanna, W.F., ed., Geologic Applications of Modern Aeromagnetic Surveys: U.S. Geological Survey Bulletin, pp: 24-45.
35. Baranov, V., 1957. A new method for interpretation of aeromagnetic maps: pseudo-gravimetric anomalies. Geophysics, 22: 359-383.
36. Baranov, V. and H. Naudy, 1964. Numerical calculation of the formula of reduction to the magnetic pole, Geophysics, 29: 67-79.
37. Bhattacharyya, B.K., 1965. Two dimensional harmonic analysis as a tool for magnetic interpretation; Geophysics, 30(5): 829-857.
38. Baranov, V., 1975. Potential fields and their transformation in applied geophysics. Geoexploration Monographs, series 1-6, Gebrüder, Borntraeger, Berlin - Stuttgart.
39. Parker, R.L., 1972. The rapid calculation of potential anomalies: Geophysical Journal of the Royal Astronomical Society, 42: 315-334.
40. Piersanti, A., C. Nostro and F. Riguzzi, 2001. Active displacement field in the Suez^Sinai area: the role of postseismic deformation, Earth and Planetary Science Letters, 193: 13-23.